Acta Crystallographica Section F
Structural Biology and Crystallization Communications
ISSN 1744-3091

Dhirendra K. Simanshu,[a] Sagar Chittori,[a] H. S. Savithri[b] and M. R. N. Murthy[a]*

[a]Molecular Biophysics Unit, Indian Institute of Science, Bangalore, India, and [b]Department of Biochemistry, Indian Institute of Science, Bangalore, India

Correspondence e-mail: mrn@mbu.iisc.ernet.in

Received 13 January 2006
Accepted 15 February 2006

Crystallization and preliminary X-ray crystallographic analysis of biodegradative threonine deaminase (TdcB) from *Salmonella typhimurium*

Biodegradative threonine deaminase (TdcB) catalyzes the deamination of L-threonine to α-ketobutyrate, the first reaction in the anaerobic breakdown of L-threonine to propionate. Unlike the biosynthetic threonine deaminase, TdcB is insensitive to L-isoleucine and is activated by AMP. Here, the cloning of TdcB (molecular weight 36 kDa) from *Salmonella typhimurium* with an N-terminal hexahistidine affinity tag and its overexpression in *Escherichia coli* is reported. TdcB was purified to homogeneity using Ni–NTA affinity column chromatography and crystallized using the hanging-drop vapour-diffusion technique in three different crystal forms. Crystal forms I (unit-cell parameters a = 46.32, b = 55.30, c = 67.24 Å, α = 103.09, β = 94.70, γ = 112.94°) and II (a = 56.68, b = 76.83, c = 78.50 Å, α = 66.12, β = 89.16, γ = 77.08°) belong to space group $P1$ and contain two and four molecules of TdcB, respectively, in the asymmetric unit. Poorly diffracting form III crystals were obtained in space group $C2$ and based on the unit-cell volume are most likely to contain one molecule per asymmetric unit. Two complete data sets of resolutions 2.2 Å (crystal form I) and 1.7 Å (crystal form II) were collected at 100 K using an in-house X-ray source.

1. Introduction

In *Escherichia coli* and *Salmonella typhimurium*, two distinctly different pyridoxal 5′-phosphate-containing L-threonine deaminases (EC 4.3.1.19) are present which catalyze the deamination of L-threonine to α-ketobutyrate (Umbarger & Brown, 1957). One of these, encoded by the gene *ilvA*, is expressed constitutively under normal growth conditions and is allosterically inhibited by the end-product of the pathway, L-isoleucine, and activated by the product of a parallel pathway, L-valine (Eisenstein, 1991). This form of threonine deaminase has been studied as the model system for investigation of feedback inhibition and allosteric regulation (Monad *et al.*, 1965; Umbarger, 1992). Since this enzyme catalyzes the first reaction in the L-isoleucine biosynthesis from L-threonine, it was called biosynthetic threonine deaminase.

A second threonine deaminase encoded by the gene *tdcB* is synthesized inside the cell when the organism is grown anaerobically in a medium containing high concentrations of amino acids and no glucose (Wood & Gunsalus, 1949). Unlike biosynthetic threonine deaminase, this enzyme is insensitive to L-isoleucine and is activated by adenosine 5′-monophosphate (AMP; Wood & Gunsalus, 1949). This enzyme catalyzes the first reaction in the anaerobic breakdown of L-threonine to propionate (Fig. 1) and is referred to as the biodegradative threonine deaminase. TdcB shares 34% sequence identity with the N-terminal domain of the biosynthetic threonine deaminase of *E. coli* and does not contain the sequence corresponding to the C-terminal regulatory domain (Gallagher *et al.*, 1998). Like the biosynthetic threonine deaminase, biodegradative threonine deaminase is expected to have a fold typical of members of the β-family of PLP-dependent enzymes (Datta *et al.*, 1987). The recently solved structure of threonine deaminase from *Thermus thermophilus* HB8 (M. Goto, unpublished result) also lacks the C-terminal domain and belongs to the fold-type II family.

Biodegradative threonine deaminase is inhibited by α-keto acids and inactivated by certain intermediary metabolites of the glycolytic

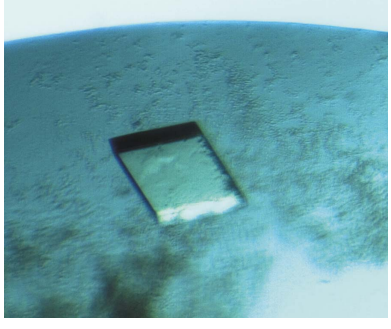

© 2006 International Union of Crystallography
All rights reserved

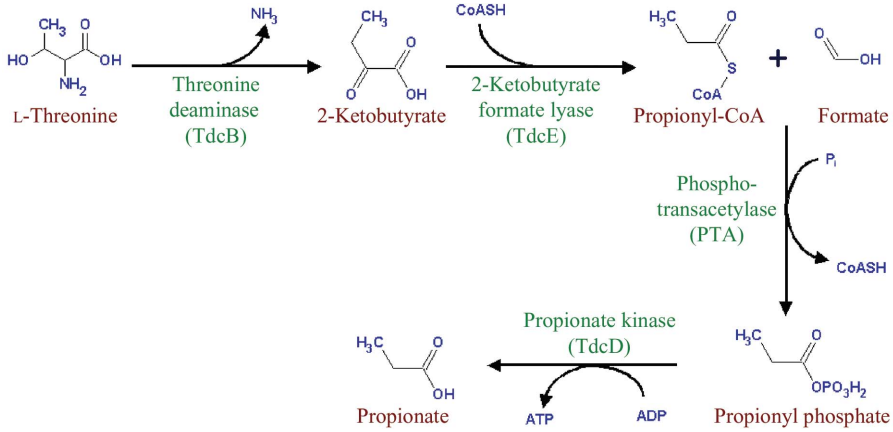

Figure 1
Metabolic pathway illustrating the anaerobic breakdown of L-threonine to propionate, in which the first reaction is catalyzed by biodegradative threonine deaminase (TdcB).

pathway and the tricarboxylic acid cycle (Bhadra & Datta, 1978; Park & Datta, 1979*a*,*b*). In TdcB, the activation of TdcB by AMP results in a large decrease in K_m for L-threonine with a small increase in V_{max} (Dunne & Wood, 1975). No evidence has been obtained for the direct participation of AMP in the reaction mechanism. AMP appears to exert its activating effect by shifting the monomer–oligomer distribution in the direction of oligomer formation (Dunne & Wood, 1975; Shizuta & Hayaishi, 1976). It is likely that during periods in which levels of energy in the cells are low, the higher concentration of AMP provides a signal for activation and conversion of L-threonine to propionate and ATP (Dunne & Wood, 1975). In *E. coli* and *S. typhimurium*, propionate can be further catabolized into pyruvate and succinate by the 2-methylcitric acid cycle (Horswill & Escalante-Semerena, 1999).

The anaerobically regulated *tdcABCDEFG* operon in *E. coli* encodes proteins involved in the transport and fermentation of L-serine and L-threonine (Sawers, 1998). Although the enzymatic conversion of L-threonine to propionate had been demonstrated as early as 1963 in cell-free extracts of *Clostridium tetanomorphum* (Tokushige *et al.*, 1963), the metabolic fate of α-ketobutyrate remained enigmatic for a long time. Recently, it was shown that in *E. coli* α-ketobutyrate is catabolized non-oxidatively into propionate (Fig. 1) by keto-acid formate lyase (TdcE), phosphotransacetylase (PTA) and propionate kinase (TdcD) (Hesslinger *et al.*, 1998).

In this paper, we report the cloning, high-level expression, purification and preliminary X-ray crystallographic studies on biodegradative threonine deaminase encoded by the *tdcB* gene from *S. enterica* serovar *typhimurium* strain IFO12529. Structure determination of biodegradative threonine deaminase will provide insight into the catalytic mechanism and ligand-induced oligomerization in this particular protein and allow direct structural comparison with the feedback-inhibited biosynthetic threonine deaminase and other members of the β-family of PLP-dependent enzymes.

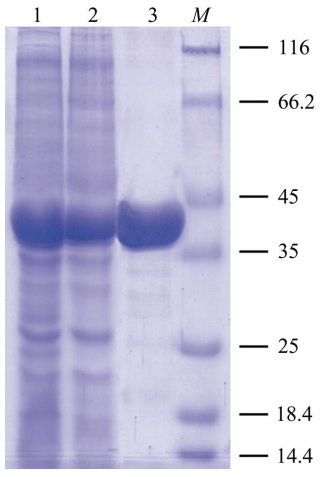

Figure 2
SDS–PAGE analysis of TdcB during purification. Proteins were analysed on 12% SDS–PAGE and stained with Coomassie blue. Lane 1, crude cell lysates after 0.3 m*M* IPTG induction; lane 2, clear supernatant; lane 3, purified TdcB after Ni–NTA affinity column chromatography; lane *M*, molecular-weight markers (kDa).

2. Materials and methods

2.1. Cloning and expression

The DNA encoding the open reading frame for biodegradative threonine deaminase (*tdcB*) was amplified using KOD HiFi DNA polymerase (Novagen) from *S. enterica* serovar *typhimurium* strain IFO 12529 genomic DNA using the polymerase chain reaction (PCR) with primers designed to introduce *Nhe*I and *Bam*HI restriction sites at the 5′ and 3′ ends, respectively. After amplification of the target gene by sense 5′-GCTAGCCATATGCACATTACATACGATCT-CCC-3′ and antisense 5′-GGATCCTTACTCGAGAGCGTCAACT-AAACCCG-3′ primers, the PCR-amplified fragment was digested with *Nhe*I and *Bam*HI and then cloned into the pRSETC vector (Invitrogen) encoding a polypeptide with an N-terminal hexahistidine tag to facilitate its purification using Ni–NTA affinity column chromatography. Thus, the final polypeptide contains the amino-acid sequence MRGSHHHHHHGMAS from the vector followed by the amino-acid sequence of TdcB starting from the second amino acid. The sequence of the *tdcB* gene was determined by nucleotide sequencing and confirmed by comparing it with the *tdcB* gene of *S. typhimurium* LT2. The plasmid was then transformed into *E. coli* strain BL21(DE3)pLysS and transformants were selected on LB agar plates containing 100 µg ml^{-1} ampicillin. Bacteria were grown overnight at 310 K in 25 ml LB broth containing ampicillin. The bacterial suspension that resulted was then diluted into fresh 2 l Terrific broth (TB) medium containing ampicillin and grown at 310 K. When the culture density (A_{600}) reached 0.6–0.7, protein expression was induced with 0.3 m*M* IPTG and cells were grown for an additional 6 h at 303 K before being harvested by centrifugation.

2.2. Purification

For the preparation of soluble protein fractions, cells from 2 l culture were resuspended in 100 ml cold lysis buffer containing 50 m*M* Tris–HCl pH 8.0, 300 m*M* NaCl and 100 µ*M* pyridoxal 5′-phosphate. The suspension was then lysed by sonication on ice. All the following purification steps were performed at 277 K. The lysate was centrifuged to remove the cell debris. The clear supernatant containing soluble proteins was gently mixed with Ni–NTA resin for 2 h and then loaded onto a glass column. Contaminating proteins were washed from the column using 50 m*M* Tris–HCl pH 8.0, 200 m*M* NaCl and 10–20 m*M* imidazole. TdcB protein was eluted from the column using 250 m*M* imidazole along with 50 m*M* Tris–HCl pH 8.0, 200 m*M* NaCl and 100 µ*M* pyridoxal 5′-phosphate. To remove imidazole, the protein was extensively dialysed against 25 m*M* Tris–HCl pH 8.0, 50 m*M* NaCl, 1 m*M* EDTA, 1 m*M* DTT and 6% glycerol. The purity of the protein was estimated using SDS–PAGE and was found to be nearly homogeneous (Fig. 2). Dialysed protein was concentrated to approximately 30 mg ml^{-1} using a 10 kDa molecular-weight cutoff Amicon Ultra-15 Centrifugal Filter Unit (Millipore) for crystallization experiments. The protein concentration was determined with Bradford reagent using bovine serum albumin as the standard protein (Bradford, 1976).

2.3. Crystallization

Crystallization conditions were screened by the hanging-drop vapour-diffusion method at 291 K using Crystal Screens I and II, SaltRx and Index Screen from Hampton Research. Crystallization drops were prepared by mixing 3 µl protein solution with 3 µl reservoir solution and were suspended over 500 µl reservoir solution in a hanging-drop vapour-diffusion setup. During screening, small crystals were obtained in crystallization conditions containing 0.1 *M* citrate buffer pH 5.6, 20% polyethylene glycol (PEG) 4000 and 20% 2-propanol (condition No. 40, Hampton Crystal Screen I) and 0.1 *M* HEPES buffer pH 7.5, 20% PEG 4000 and 10% 2-propanol (condition No. 41, Hampton Crystal Screen I). Further optimization of these two conditions was carried out by varying the pH and the molecular weight of the PEG and using various organic solvents. 10–15% 2-propanol along with citrate buffer in the pH range 5.6–6.5 and 20–25% PEG 3350 or PEG 4000 gave good diffraction-quality crystals. Both PEG 3350 and PEG 4000 gave apparently equivalent results. Of the various organic solvents screened, substitution of 2-propanol by either 10–15% *t*-butanol or 0.6–0.9 *M* 1,6-hexanediol gave diffraction-quality crystals of different crystal forms (Fig. 3). Crystals obtained in the presence of 10–15% *t*-butanol diffracted better than those obtained in the presence of 2-propanol. Yet another crystal form of TdcB obtained in the presence of 0.6–0.9 *M* 1,6-hexanediol diffracted very poorly in the resolution range 4–5 Å. The two crystal forms for which diffraction data are reported in this manuscript were obtained from conditions containing 0.1 *M* citrate buffer pH 6.0, 20% PEG 3350 and 10% 2-propanol (crystal form I) and 0.1 *M* citrate buffer pH 6.0, 20% PEG 3350 and 15% *t*-butanol (crystal form II). These crystals appeared after 5 d of equilibration against the crystallization solution and grew to full size in 10 d.

Table 1
Data-collection statistics.

Values in parentheses correspond to the last resolution shell.

	Crystal form I	Crystal form II
Resolution range (Å)	30.0–2.2 (2.28–2.20)	30.0–1.7 (1.76–1.70)
Space group	*P*1	*P*1
Temperature (K)	100	100
Unit-cell parameters		
a (Å)	46.32	56.68
b (Å)	55.30	76.83
c (Å)	67.24	78.50
α (°)	103.09	66.12
β (°)	94.70	89.16
γ (°)	112.94	77.08
Total No. of reflections	360350	2012989
No. of unique reflections	29556	128680
Completeness (%)	94.7 (84.5)	93.1 (86.9)
Mosaicity (°)	0.89	0.75
Data redundancy	12.19	15.64
No. of molecules per ASU	2	4
V_M (Å^3 Da^{-1})	2.0	2.1
Solvent content (%)	40.0	40.1
Average $I/\sigma(I)$	22.18 (4.98)	26.58 (2.76)
R_{merge}† (%)	5.3 (22.2)	4.1 (42.6)

† $R_{merge} = \sum_j \sum_h |I_{hj} - \langle I_h \rangle| / \sum_j \sum_h \langle I_{hj} \rangle$, where I_{hj} is the jth measurement of the intensity of reflection h and $\langle I_h \rangle$ is the average intensity.

2.4. Data collection

A complete data set for each crystal form was collected using a single crystal of the respective crystal form at 100 K. The crystals were transferred to a cryoprotectant composed of reservoir solution with 20% ethylene glycol prior to mounting. X-ray diffraction data were collected using a MAR Research image-plate system (diameter 345 mm) with Osmic mirrors and a Rigaku RU-200 rotating-anode X-ray generator with a 300 µm focal cup. Data were indexed, integrated and scaled using *DENZO* and *SCALEPACK* as implemented in the *HKL*2000 suite (Otwinowski & Minor, 1997). The final statistics for data collection and processing are summarized in Table 1.

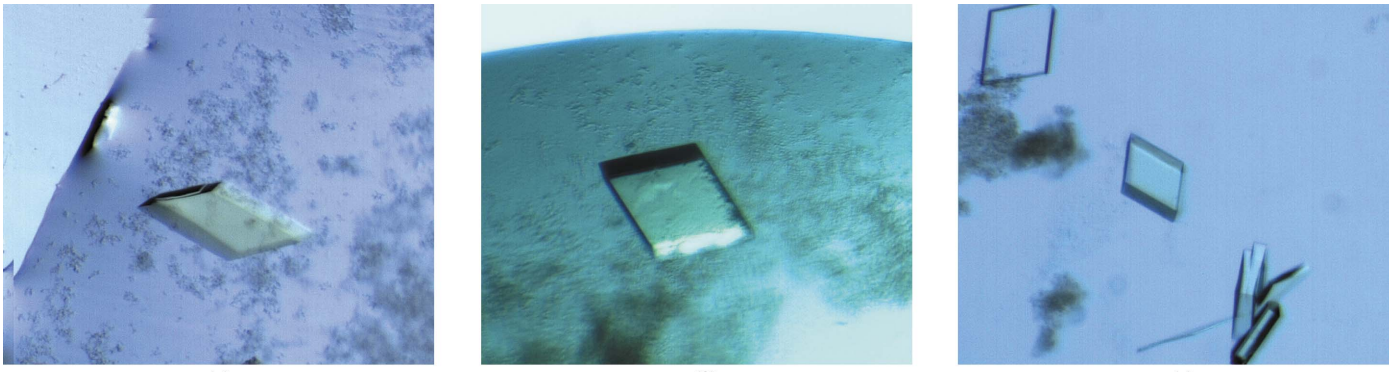

(*a*) (*b*) (*c*)

Figure 3
Crystals of TdcB obtained in three different crystal forms in the presence of crystallization conditions containing (*a*) 2-propanol (crystal form I), (*b*) *t*-butanol (crystal form II) and (*c*) 1,6-hexanediol (crystal form III).

3. Results and discussion

TdcB was successfully cloned in the pRSETC vector (Invitrogen) with an N-terminal hexahistidine tag and was purified using Ni–NTA affinity column chromatography. By transforming the plasmid into *E. coli* strain BL21(DE3)pLysS, recombinant protein was expressed at a level of about 25 mg in 1 l TB medium. Prior to crystallization, the protein was concentrated to 30 mg ml^{-1}. Crystallization trials were performed using crystallization screens available from Hampton Research, which produced initial crystals. A fine screen that included variations in pH, precipitant and organic solvents yielded well ordered diffraction-quality crystals. Three different organic solvents, 2-propanol, *t*-butanol and 1,6-hexanediol, along with 0.1 *M* citrate buffer in the pH range 5.6–6.5 and 20–25% PEG 3350 or PEG 4000 resulted in diffraction-quality crystals in three different crystal forms. Form I crystals belonged to space group *P*1, with a Matthews coefficient of 2.0 Å^3 Da^{-1}, corresponding to a solvent content of 40.0% with two molecules of TdcB in the asymmetric unit (Matthews, 1968). Form II crystals also belonged to space group *P*1, with a Matthews coefficient of 2.1 Å^3 Da^{-1}, corresponding to a solvent content of 40.1%, and contained four molecules of TdcB in the asymmetric unit (Matthews, 1968) (Table 1). Form III crystals, which only diffracted to a resolution of 4–5 Å, belonged to space group *C*2, with unit-cell parameters $a = 52.66$, $b = 74.64$, $c = 77.58$ Å, $\beta = 96.10^\circ$. Based on the unit-cell volume, it is most likely to contain one molecule of TdcB in the asymmetric unit, with a Matthews coefficient of 2.1 Å^3 Da^{-1} (Matthews, 1968), corresponding to a solvent content of 41.3%. Attempts to improve the resolution of form III crystals have so far been unsuccessful.

Since TdcB shares sequence identity of 34 and 35%, respectively, with the N-terminal domain (residues 5–333) of biosynthetic threonine deaminase from *E. coli* (PDB code 1tdj) and threonine deaminase from *T. themophilus* HB8 (PDB code 1ve5; M. Goto, unpublished results), the atomic coordinates of both the proteins, with non-identical residues converted to alanine, were used separately as search models for the structure solution of TdcB by molecular replacement with the program *AMoRe* (Navaza, 1994). Because of the high resolution, crystal form II data in the 15.0–3.0 Å resolution range were used for the rotation and translation searches. The top solution from the rotation function was used in the translation search to locate the first of the four molecules. When all four molecules were positioned, the highest peak of translation had a correlation coefficient of 47.2% and an *R* factor of 55.6% with the N-terminal domain of biosynthetic threonine deaminase of *E. coli* as the search model and a correlation coefficient of 46.2% and an *R* factor of 56.9% using the thermophilic threonine deaminase as the search model. In both the cases, examination of the best solution revealed good crystal packing and no clashes between symmetry-related molecules. The best molecular-replacement solution was used for further refinement using program *REFMAC* from the *CCP*4 suite (Murshudov *et al.*, 1997; Collaborative Computational Project, Number 4, 1994). Initial phases for crystal form I were obtained using a monomer of crystal form II as the search model. Model building and refinement of these two crystal forms are presently in progress.

The intensity data were collected at the X-ray Facility for Structural Biology at the Molecular Biophysics Unit, Indian Institute of Science, supported by the Department of Science and Technology (DST) and the Department of Biotechnology (DBT) of the Government of India. We thank Mr Babu and Mr James Paul for their cooperation during the course of data collection. MRNM and HSS acknowledge financial support from DST and DBT. DKS acknowledge the Council for Scientific and Industrial Research, Government of India for the fellowship.

References

Bhadra, R. & Datta, P. (1978). *Biochemistry*, **17**, 1691–1699.
Bradford, M. M. (1976). *Anal. Biochem.* **72**, 248–254.
Collaborative Computational Project, Number 4 (1994). *Acta Cryst.* D**50**, 760–763.
Datta, P., Goss, T. J., Omnaas, J. R. & Patil, R. V. (1987). *Proc. Natl Acad. Sci. USA*, **84**, 393–397.
Dunne, C. P. & Wood, W. A. (1975). *Curr. Top. Cell. Regul.* **9**, 65–101.
Eisenstein, E. (1991). *J. Biol. Chem.* **266**, 5801–5807.
Gallagher, D. T., Gilliland, G. L., Xiao, G., Zondlo, J., Fisher, K. E., Chinchilla, D. & Eisenstein, E. (1998). *Structure*, **6**, 465–475.
Hesslinger, C., Fairhurst, S. A. & Sawers, G. (1998). *Mol. Microbiol.* **27**, 477–492.
Horswill, A. R. & Escalante-Semerena, J. C. (1999). *J. Bacteriol.* **181**, 5615–5623.
Matthews, B. W. (1968). *J. Mol. Biol.* **33**, 491–497.
Monad, J., Wyman, J. & Changeux, J. P. (1965). *J. Mol. Biol.* **12**, 88–118.
Murshudov, G. N., Vagin, A. A. & Dodson, E. J. (1997). *Acta Cryst.* D**53**, 240–255.
Navaza, J. (1994). *Acta Cryst.* A**50**, 157–163.
Otwinowski, Z. & Minor, W. (1997). *Methods Enzymol.* **276**, 307–326.
Park, L. S. & Datta, P. (1979*a*). *J. Bacteriol.* **138**, 1026–1028.
Park, L. S. & Datta, P. (1979*b*). *J. Biol. Chem.* **254**, 7927–7934.
Sawers, G. (1998). *Arch. Microbiol.* **171**, 1–5.
Shizuta, Y. & Hayaishi, O. (1976). *Curr. Top. Cell Regul.* **11**, 99–146.
Tokushige, M., Whiteley, H. R. & Hayaishi, O. (1963). *Biochem. Biophys. Res. Commun.* **171**, 1319–1325.
Umbarger, H. E. (1992). *Protein Sci.* **1**, 1392–1395.
Umbarger, H. E. & Brown, B. (1957). *J. Bacteriol.* **73**, 105–112.
Wood, W. A. & Gunsalus, I. C. (1949). *J. Biol. Chem.* **181**, 171–182.